C. Kennard & R.J. Leigh (Eds.)
Progress in Brain Research, Vol. 171
ISSN 0079-6123

CHAPTER 1.7

Acute superior oblique palsy in the monkey: effects of viewing conditions on ocular alignment and modelling of the ocular motor plant

Christian Quaia[1], Xiaoyan Shan[2], Jing Tian[2], Howard Ying[2], Lance M. Optican[1], Mark Walker[3], Rafael Tamargo[2] and David S. Zee[2,*]

[1]*Laboratory of Sensorimotor Research, National Eye, Institute, Bethesda, MD, USA*
[2]*Department of Neurology, The Johns Hopkins Hospital, 600 N. Wolfe St., Baltimore, MD, USA*
[3]*Case Western Reserve University, Cleveland, OH, USA*

Abstract: We investigated the immediate and long-term changes in static eye alignment with acute superior oblique palsy (SOP) in the monkey. When the paretic eye was patched immediately after the lesion for 6–9 days, vertical alignment slowly *improved*. When the patch was removed and binocular viewing was allowed, alignment slowly *worsened*. In contrast when a monkey was not patched immediately after the lesion vertical alignment did not improve. We also show that a model of the eye plant can reproduce the observed acute deficit induced by SOP, but only by abandoning Robinson's symmetric simplification of the reciprocal innervation relationship within pairs of agonist–antagonist muscles. The model also demonstrated that physiologic variability in orbital geometry can have a large impact on SOP deficits.

Keywords: superior oblique palsy; strabismus; eye plant; ocular motor; adaptation; eye movements

Introduction

In human patients with strabismus, vertical misalignment of the eyes that is more pronounced when the higher eye is in adduction is usually attributed to a palsy of the superior oblique muscle (SOP). In many patients, however, it is difficult to reliably differentiate a 'congenital' from an acquired SOP. Furthermore, orbital imaging suggests that many patients with a presumed congenital SOP do not have a trochlear (IV) nerve palsy but rather an anatomical abnormality in the orbit that mimics SOP (Chan and Demer, 1999). And even when the evidence points to a complete trochlear nerve palsy, the degree and pattern of the static deviations are variable (Graf et al., 2005; Khawam et al., 1967). Inherent variation in the anatomical configuration of the SO muscle and tendon (Fink, 1962; Helveston et al., 1992), secondary changes in the mechanical properties of the palsied muscle and its antagonists (Robinson, 1985; Jampolsky, 1994; Scott, 1994), and central adaptive processes (Maxwell and Schor, 2006) all conspire against a correct diagnosis.

To provide a frame of reference for analysing the clinical presentation of both acute and chronic SOP in humans, and to gather experimental data for developing better models of the eye plant, we

*Corresponding author. Tel.: +1 410 955 3319;
Fax: +1 216 231 3461; E-mail: dzee@dizzy.med.jhu.edu

DOI: 10.1016/S0079-6123(08)00607-9

developed an experimental monkey model of acute SOP using intracranial trochlear nerve section (Shan et al., 2007). We sought to isolate the deficit caused by muscle palsy, and to determine what changes in the alignment of the eyes might occur afterwards. Two surprising findings emerged from this study (Fig. 1). First, when the animals (M1 and M2) wore a patch in front of the palsied eye during the days immediately after the IV nerve section, the vertical misalignment gradually *decreased* over days (left arrow). Second, once the eye patch was removed and binocular vision was allowed, the vertical misalignment *worsened* again, and even exceeded the initial deficit (right arrow).

These findings point to a critical influence of the pattern of habitual viewing (out of one eye or both) on ocular alignment just after the onset of an acute paralytic strabismus. We speculated that the early improvement in alignment during habitual monocular viewing was mediated by signals from the *proprioceptors* in the paretic eye, and that the subsequent deterioration was driven, at least in part, by overriding central mechanisms. Here we present some new findings that confirm the importance of the habitual state of viewing (monocular versus binocular) in the early changes in alignment after acute trochlear nerve palsy. We also present preliminary modelling results that help explain the patterns of misalignment observed with SOP.

Effects of viewing conditions on ocular misalignment

To test the hypothesis that monocular viewing mediates the adaptive mechanism that reduces the vertical misalignment, in a new experiment (monkey M3), instead of patching the paretic eye immediately after the surgery, we allowed uninterrupted binocular vision after the trochlear nerve section (Fig. 2). The result was clear cut: No improvement occurred during the early period after the lesion (left arrow) and, as was the case with the previous animals when binocular viewing was allowed after a period of patching, the misalignment worsened over time (right arrow). These data support the idea that (regardless of mechanism) monocular viewing after a paralytic strabismus is the factor leading to the initial decrease in ocular misalignment, and late increases in misalignment can occur even when the animal has not been patched immediately post-lesion.

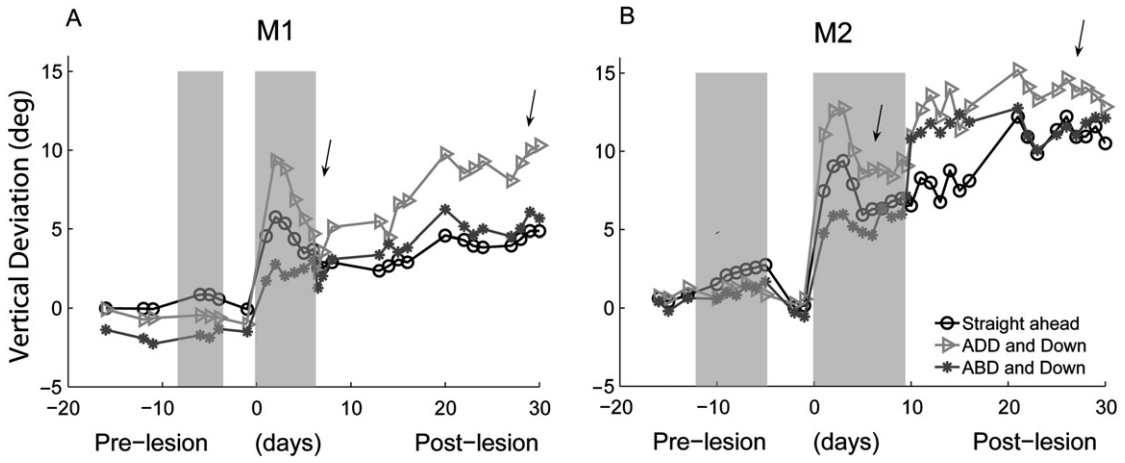

Fig. 1. Time course of vertical deviation with normal eye viewing pre- and up to 30 days post-SOP for M1 (A) and M2 (B). Shaded area: The paretic eye (or to-be-paretic eye) habitually patched. Positive deviation indicates that the paretic eye is relatively higher. Lesion was induced on day zero. ADD: Paretic eye in adduction (normal eye in abduction), ABD: paretic eye in abduction (normal eye in adduction). Left arrow indicates lessening misalignment while the animals were patched and right arrows indicate increasing misalignment after binocular viewing was allowed. Adapted with permission from Shan et al. (2007).

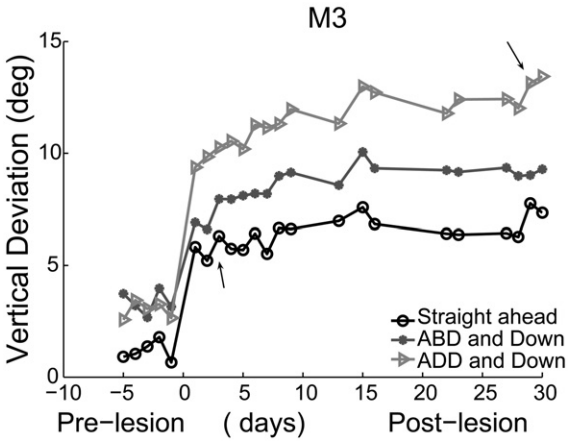

Fig. 2. Vertical deviation of M3 (NEV). Lesion is at day 0. After the lesion about 5 degrees of vertical deviation develops in the straight ahead position, and slightly more in the adducted, down position. Note that prior to the lesion there was a vertical phoria of a few degrees in the down positions probably related to mild restriction in the to-be-paretic eye in down gaze. The upward directed arrow (left) indicates the lack of improvement in alignment during the early days after the lesion and the downward directed arrow (right) indicates that there is some increase in misalignment over time.

Mathematical simulations of ocular motor behaviour

The characterization of the immediate effect of SOP allowed us to effectively validate a mathematical model of the eye plant. To this end we adapted our previously published model of the human eye plant (Quaia and Optican, 2003) to the geometry of the monkey orbit. The measures for the origin and the insertions of the muscles on the eyeball, and the location of the trochlea, were based on Suzuki et al. (1999). The relative strength of each muscle was estimated using two measures: their cross-section (Miller and Robins, 1987) and the number of fibres in the global layer (Oh et al., 2001; Kono et al., 2005). These measures provided us with a fairly tight range of values, but also indicated the importance of future direct experimental measurements.

The functional locations of the pulleys are not known in monkeys, and so we arranged them as follows: the pulleys for the LR and MR were placed at the same coordinates in the coronal plane as their insertions, but they were posterior to the globe centre by 80% of the anterior location of the (respective) muscle insertion. The rationale for this criterion is that in elevation the axis of action of the LR tips back (i.e., gains a torsional component) by a little more than half the elevation angle (Klier et al., 2006), indicating that its inflection point is slightly less posterior than its insertion is anterior (relative to the eye centre). The pulleys for the SR and IR were placed along the path that each muscle would travel with the eye in primary position if there were no pulleys, and at a distance from the insertion that is twice the anterior location of the insertion. This criterion was selected because this appears to be the arrangement in the human orbit (i.e., whereas in primary position there is a fairly clear inflection point for the horizontal recti, the vertical recti largely travel along the shortest path from origin to insertion). We placed the IO pulley: (1) at the same elevation as the IR pulley; (2) laterally between the LR and IR pulleys, but closer to the IR pulley; and (3) half-way between the posterior locations of the LR and IR pulleys. This placed the pulley for the IO between the pulleys for the LR and the IR, as is for humans (Demer et al., 2003). In addition, we have also allowed the pulleys to move as the eye rotates, in accordance with the active pulleys hypothesis (Demer, 2006). The amount of movement of the pulleys for the recti muscles has been inferred from Kono et al. (2002) and Clark et al. (1997), and the amount of motion of the IO pulley is based on Demer et al. (2003). This pattern is compatible with the coordinated pulley hypothesis (Miller, 2007). Because that data refers to a human plant, the amount of motion per degree of eye rotation was scaled down to account for the smaller radius of the eye in monkeys. Using these parameters the length and axis of action of each muscle were computed as a function of the orientation of the eye, and length–tension–innervation equations (Robinson, 1975) were used to compute the muscle force as a function of muscle length and innervation.

Simulating a SOP is then quite simple: first, one needs to solve the *inverse control problem*, i.e., determine the muscle innervations required to hold

the orientation of the healthy eye. Then, the innervation to the model superior oblique is forced to zero, thus simulating the effect of a SOP. Since Robinson's original SQUINT model (Robinson, 1975), all mathematical models of the plant have solved the inverse control problem by imposing a specific relationship between the innervation supplied to two muscles in an agonist–antagonist pair. This relationship was always described using a *symmetric* hyperbola. However, when we used this approach the model failed to reproduce the observed results, predicting instead much smaller deficits. No adjustment of the parameters described above (within a physiologic range) improved matters. This might explain why when plant models have been used to replicate the deficit observed in humans with SOP, they had to invoke secondary muscular or adaptive changes (Miller and Demer, 1992; Porrill et al., 2000; Straumann et al., 2003; Haslwanter et al., 2005).

It turns out that the reciprocal innervation formulation is the culprit, as there is no reason to believe that the reciprocal relationship is symmetric. The only reasonable constraint is that it is reciprocal (i.e., if the innervation to one muscle goes up, the innervation to the other goes down, as Sherrington originally proposed). We could actually prove this idea because the length–tension–innervation curve measured by Robinson provides all the information needed to estimate the actual relationship in the horizontal recti (in humans). Using Robinson's original data, the relationship between the innervation in the lateral and medial recti was actually *asymmetric*. Accordingly, we removed the symmetric constraint from our model, and used the data from the SO palsy to directly estimate this relationship for the oblique muscles, as shown in the flow chart. This procedure was run by an optimization algorithm until the best fit was obtained. The final result (Fig. 3) closely fit the behaviour of the two monkeys, and their derived SO/IO innervation relationships (step 6, flow chart) were similar.

In an effort to uncover potential sources of variability in the effects induced by SOP, we have begun examining the sensitivity of our model to changes in orbital parameters. We first examined the angle of insertion of the SO tendon on the globe, a parameter that varies considerably among human subjects (Fink, 1962). We changed the angle by $\pm 30^{\circ}$ relative to its average insertion (which covers the range reported by Fink in humans), and then applied our simulation algorithm to the modified plant model (Fig. 4). For

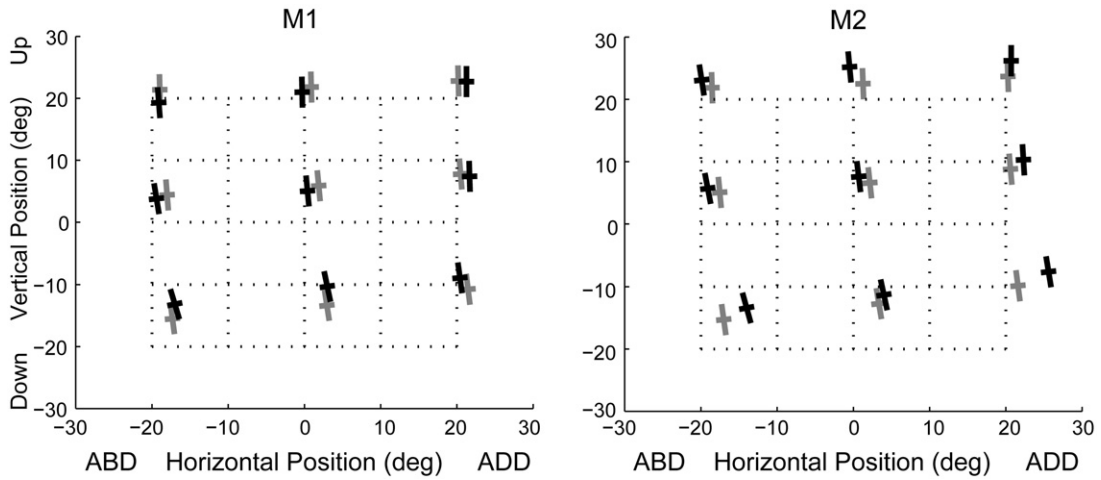

Fig. 3. Simulations for M1 and M2 (left SOP). Grey symbols are simulations and black symbols are monkey data. Shown is paretic eye (PE) position. Fixation points for normal eye are $\pm 20^{\circ}$ and straight ahead. ADD/ABD refer to PE position. Data are corrected for pre-lesion phorias with same period of patching as post-lesion (2–3 days). Tilt of vertical lines reflects torsional phoria. The simulations capture well the gradients and amplitudes of the vertical and torsional deviations.

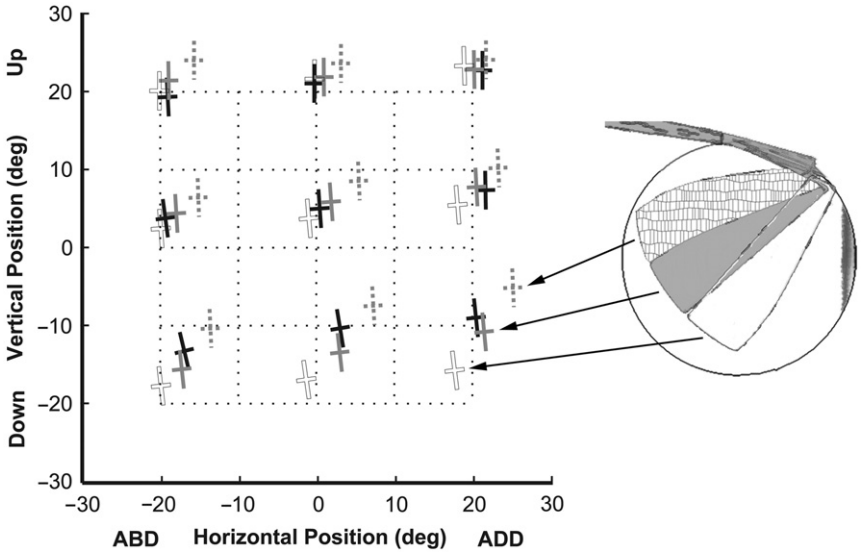

Fig. 4. Simulations of SOP. Black solid crosses: Monkey data (M1). Grey solid crosses: Standard insertion location. Open crosses: $+30^{\circ}$ insertion; dashed crosses: -30° insertion. See right panel for SO tendon path for each insertion location (right eye, seen from above). Note the considerable effect of moving the insertion on the predicted misalignment (vertical, torsional, and horizontal) especially in down gaze. As expected there is a reciprocal relationship between torsion and vertical misalignment, but note also the considerable variation in the horizontal misalignment (even to the point of a small exodeviation).

Table 1. Simulation flow chart

1. Guess the common-mode innervations (i.e., average of the innervations in an agonist–antagonist pair) (asymmetric parabola).
2. Find a set of differential innervations (i.e., difference between innervations in a pair) to keep the intact eye in each of the nine fixation positions.
3. Set the innervation of SO to zero.
4. Change the innervation of the IO to match the positions of the paretic eye.
5. Change the innervation of the SO to match the positions of the normal eye.
6. Fit new innervations for the SO and IO for the nine fixation positions to an asymmetric parabola to estimate reciprocal innervation of SO/IO. This will be unique to each animal.
7. Find a new set of innervations to keep the intact eye in each of the nine fixation positions.
8. Set the innervation of the SO to zero (create a SOP).
9. Compare the alignment of the monkey with the model.

each insertion angle, we repeated the procedure in Table 1. From these simulations we note that in spite of the degrees of freedom of the model, only the original model provides a good fit across the nine positions tested and that orbital geometry can have a large impact on the outcome of the lesion (e.g., compare the difference between the two anatomical variations especially in down gaze). This finding implies that, not surprisingly, orbital geometry can be an important determinant of the variability observed in patients, and suggests that attempts to measure the location of the insertion of the SOP in our animals (e.g., with post mortem anatomical evaluations) will be worthwhile. Also, this suggests that our model and strategy of simulation are reasonable, as a somewhat different geometry would have resulted in a considerably worse fit. In other words, the number of degrees of freedom is not so high as to render the simulations without significance, as would have been the case if changes in the reciprocal innervation patterns had enabled the model to always reproduce the deficit observed, regardless of geometry.

References

Chan, T.K. and Demer, J.L. (1999) Clinical features of congenital absence of the superior oblique muscle as demonstrated by orbital imaging. J. AAPOS, 3(3): 143–150.

Clark, R.A., Miller, J.M. and Demer, J.L. (1997) Location and stability of rectus muscle pulleys: muscle paths as a function of gaze. Invest. Ophthalmol. Vis. Sci., 38(1): 227–240.

Demer, J.L. (2006) Current concepts of mechanical and neural factors in ocular motility. Curr. Opin. Neurol., 19(1): 4–13.

Demer, J.L., Oh, S.Y., Clark, R.A. and Poukens, V. (2003) Evidence for a pulley of the inferior oblique muscle. Invest. Ophthalmol. Vis. Sci., 44(9): 3856–3865.

Fink, W.H. (1962) Surgery of the vertical muscles of the eye. Thomas, Springfield, IL.

Graf, M., Krzizok, T. and Kaufmann, H. (2005) Head-tilt test in unilateral and symmetric bilateral acquired trochlear nerve palsy (in German). Klin. Monatsbl. Augenheilkd., 222: 142–149.

Haslwanter, T., Buchberger, M., Kaltofen, T., Hoerantner, R. and Priglinger, S. (2005) SEE + +: a biomechanical model of the oculomotor plant. Ann. N.Y. Acad. Sci., 1039: 9–14.

Helveston, E.M., Krach, D., Plager, D.A. and Ellis, F.D. (1992) A new classification of superior oblique palsy based on congenital variations in the tendon. Ophthalmology, 99(10): 1609–1615.

Jampolsky, A. (1994) A new look at the head tilt test. In: Fuchs A.F., Brandt T.h., Büttner U. and Zee D.S. (Eds.), Contemporary Oculomotor and Vestibular Research: A Tribute to David A. Robinson. Thieme Verlag, Stuttgart, pp. 432–439.

Khawam, E., Scott, A.B. and Jampolsky, A. (1967) Acquired superior oblique palsy. Diagnosis and management. Arch. Ophthalmol., 77(6): 761–768.

Klier, E.M., Meng, H. and Angelaki, D.E. (2006) Three-dimensional kinematics at the level of the oculomotor plant. J. Neurosci., 26(10): 2732–2737.

Kono, R., Clark, R.A. and Demer, J.L. (2002) Active pulleys: magnetic resonance imaging of rectus muscle paths in tertiary gazes. Invest. Ophthalmol. Vis. Sci., 43(7): 2179–2188.

Kono, R., Poukens, V. and Demer, J.L. (2005) Superior oblique muscle layers in monkeys and humans. Invest. Ophthalmol. Vis. Sci., 46(8): 2790–2799.

Maxwell, J.S. and Schor, C.M. (2006) The coordination of binocular eye movements: vertical and torsional alignment. Vision Res., 46(21): 3537–3548.

Miller, J.M. (2007) Understanding and misunderstanding extraocular muscle pulleys. J. Vis., 7(11): 1–15.

Miller, J.M. and Demer, J.L. (1992) Biomechanical analysis of strabismus. Binoc. Vis. Eye Muscle Surg. Quart., 7: 233–248.

Miller, J.M. and Robins, D. (1987) Ocular muscle sideslip and orbital geometry in monkeys. Vision Res., 27(3): 381–392.

Oh, S.Y., Poukens, V., Cohen, M.S. and Demer, J.L. (2001) Structure-function correlation of laminar vascularity in human rectus extraocular muscles. Invest. Ophthalmol. Vis. Sci., 42(1): 17–22.

Porrill, J., Warren, P.A. and Dean, P. (2000) A simple control law generates Listing's positions in a detailed model of the extraocular muscle system. Vision Res., 40: 3743–3758.

Quaia, C. and Optican, L.M. (2003) Dynamic eye plant models and the control of eye movements. Strabismus, 11(1): 17–31.

Robinson, D.A. (1975) A quantitative analysis of extraocular muscle cooperation and squint. Invest. Ophthalmol., 14(11): 801–825.

Robinson, D.A. (1985) Bielschowsky head-tilt test. II. Quantitative mechanics of the Bielschowsky head-tilt test. Vision Res., 25(12): 1983–1988.

Scott, A.B. (1994) Change of eye muscle sarcomeres according to eye position. J. Pediatr. Ophthalmol. Strab., 31(2): 85–88.

Shan, X., Tian, J., Ying, H., Quaia, C., Optican, L., Walker, M., Tamargo, R. and Zee, D.S. (2007) Acute superior oblique palsy in monkeys: I. Changes in static eye alignment. Invest. Ophthalmol. Vis. Sci., 48(6): 2602–2611.

Straumann, D., Steffen, H., Landau, K., Bergamin, O., Mudgil, A.V., Walker, M.F., Guyton, D.L. and Zee, D.S. (2003) Primary position and Listing's law in acquired and congenital trochlear nerve palsy. Invest. Ophthalmol. Vis. Sci., 44(10): 4282–4292.

Suzuki, Y., Straumann, D., Simpson, J.I., Hepp, K., Hess, B.J. and Henn, V. (1999) Three-dimensional extraocular motoneuron innervation in the rhesus monkey. I: muscle rotation axes and on-directions during fixation. Exp. Brain Res., 126(2): 187–199.